



# Multimodal neuroimaging insights into the neurobiology of healthy aging across the lifespan

Laust Vind Knudsen<sup>1</sup> · Tanja Maria Michel<sup>1</sup> · Ziba Ahangarani Farahani<sup>2</sup> · Manouchehr Seyedi Vafaei<sup>1</sup>

Received: 30 September 2024 / Accepted: 16 January 2025 / Published online: 1 February 2025  
© The Author(s) 2025

## Abstract

**Purpose** The purpose of this study was to advance our understanding of the neurobiology of healthy aging, which is crucial for improving quality of life and preventing age-related diseases. Despite its importance, a comprehensive investigation of this process has yet to be fully characterized.

**Methods** We used a hybrid PET/MRI scanner to assess neurophysiological parameters in 80 healthy individuals aged 20–78. Cerebral amyloid-beta ( $A\beta$ ) deposition and glucose metabolism were assessed using PET scans, while participants underwent simultaneous MRI scans.

**Results** We found a positive correlation between  $A\beta$ -deposition and aging, and a negative correlation between glucose metabolism and aging. The insula showed the strongest negative correlation between glucose metabolism and age (Spearman's  $r = -0.683$ , 95% CI  $[-0.79, -0.54]$ ,  $p < 0.0001$ ), while the posterior cingulate cortex had the strongest positive correlation between  $A\beta$ -deposition and age (Spearman's  $r = 0.479$ , 95% CI  $[0.28, 0.64]$ ,  $p < 0.0001$ ). These results suggest a spatially dependent link between  $A\beta$ -deposition and metabolism in healthy older adults, indicating a compensatory mechanism in early Alzheimer's. Additionally,  $A\beta$ -deposition was linked to changes in interregional neural communication.

**Conclusions** Our study confirms previous findings on aging and offers new insights, particularly on the role of  $A\beta$ -deposition in healthy aging. We observed a linear increase in  $A\beta$ -deposition, alongside decreases in white matter integrity, cerebral blood flow, and glucose metabolism. Additionally, we identified a complex regional relationship between  $A\beta$ -deposition, glucose metabolism, and neural communication, possibly reflecting compensatory mechanisms.

**Keywords** PET · MRI · Glucose metabolism · Amyloid-beta · Functional connectivity · Aging

## Introduction

Aging is a gradual process starting in adulthood, with bodily functions declining by middle age [1]. The brain, a key target, experiences reduced neurogenesis, mitochondrial issues, impaired metabolism, oxidative stress, and cognitive decline [2]. The reduction of neurotransmitters [3, 4] and increased amyloid-beta ( $A\beta$ ) plaques are key factors in

aging and related neurological disorders [5]. Brain energy is mainly provided by glucose metabolism [6]. Molecular imaging studies show that while cerebral blood flow (CBF) may vary with age [7], cerebral metabolic rate of glucose (CMRglc) decline more significantly in disorders like Alzheimer's disease (AD) than in healthy aging [8]. AD is a global healthcare issue, with cases expected to reach 153 million by 2050 due to aging populations [9]. The amyloid cascade hypothesis proposed by Hardy and Higgins [10], supported by genetic and imaging studies, suggests that AD results from abnormal  $A\beta$ -plaque buildup in the brain, leading to neurofibrillary tangles and cell death.  $A\beta$ -plaques may start accumulating 20 years before symptoms, followed by tau aggregates and neurodegeneration [11]. Significant levels of  $A\beta$  are found in healthy older individuals without evidence of clinically apparent cognitive decline [12], as a result imaging of  $A\beta$ -deposition could be a promising tool for early diagnosis and treatment assessment. The Pittsburgh

---

Tanja Maria Michel Shared first author.

---

✉ Manouchehr Seyedi Vafaei  
mvafaei@health.sdu.dk

<sup>1</sup> Department of Psychiatry, University of Southern Denmark, Odense University Hospital, Odense C 5000, Denmark

<sup>2</sup> Department of Nuclear Medicine, Odense University Hospital, Odense C 5000, Denmark

Compound-B ( $[^{11}\text{C}]\text{-PiB}$ ) is ideal for positron emission tomography (PET) to assess  $\text{A}\beta$ -deposition [13]. Imaging studies show early  $\text{A}\beta$  buildup in the cingulate, orbitofrontal, and precuneus regions of cognitively healthy older adults [14–16]. However,  $\text{A}\beta$ -deposition across the lifespan remains understudied, with only one study exploring it in healthy individuals of varying ages [5]. This study aimed to examine the relationship between age and  $\text{A}\beta$ -deposition, as well as its spatial distribution. Additionally, it investigated the effects of  $\text{A}\beta$ -deposition on CMRglc, CBF, functional connectivity (FC), and white matter integrity. The proposed studies aimed to test hypotheses linking mechanisms of brain aging, including: (1)  $\text{A}\beta$ -deposition increases with age while glucose metabolism declines, and these are inversely related; (2)  $\text{A}\beta$  affects both increased and decreased functional connectivity in the default mode network; (3) white matter integrity worsens with age and  $\text{A}\beta$ -deposition; (4) CBF declines with age and is negatively impacted by  $\text{A}\beta$ -deposition. To achieve this, PET, in conjunction with functional MRI (fMRI), diffusion MRI (dMRI), and arterial spin labeling (ASL), were used to measure and analyse these changes. This approach allowed us to measure and correlate changes in these variables in the aging brain, offering insights into their interactions during healthy aging and highlighting potential disruptions.

## Materials and methods

### Participants

Initially, 83 subjects were recruited through a company for research subject recruitment. The recruitment and scans were performed from January 2021 until September 2023. The scans were performed at the Nuclear Medicine department of Odense University Hospital in Denmark. Following an introductory telephone conversation outlining the scanning procedure, participants provided documentation from their personal physician confirming their neurological and psychiatric health status, otherwise they were excluded. Additionally, participants were excluded if they were using any prescription medication, except for over-the-counter remedies such as cold medicine or temporary pain relievers, if younger than 20 years, and if not fasted >6 h before the scan. On the day of the scan, a physician conducted a brief health assessment for all participants to ensure their well-being. Two subjects were excluded from the study due to suspicious MRI scans. A total of 83 healthy participants underwent simultaneous PET and MRI scans. Among them, 81 PiB scans and 79 FDG ( $[2\text{-}[^{18}\text{F}]\text{-fluoro-2-deoxy-D-glucose}]\text{-FDG}$ ) scans were without structural abnormalities and of adequate image quality. One subject (aged 70) showed

unusually high  $\text{A}\beta$  deposition, approximately double that of age-matched individuals, and was excluded as an outlier using the Interquartile Range method. This exclusion was necessary because our study focuses on  $\text{A}\beta$  deposition in normal aging, and the elevated SUVR in this individual likely indicates early-stage AD. Consequently, the present study includes 80 participants (See Table in Online Resource 1).

### Data acquisition and image processing

Participants were scanned using a 3.0T GE Healthcare SIGNA<sup>TM</sup> PET/MR system (GE Healthcare, Chicago, IL, USA) equipped with a 19-channel head-and-neck unit. Attenuation-correction maps were generated using GE zero-echo-time based correction for PET/MRI brain imaging. Initially participants underwent a  $^{11}\text{C}\text{-PiB}$  PET scan. After a delay of five half-lives of this tracer,  $^{18}\text{F}\text{-FDG}$  was administered for the subsequent scan. Simultaneously structural T1-weighted MRI, fMRI, dMRI and ASL data were collected. Comprehensive details regarding the scanner acquisition parameters for PET and MRI are provided in Online Resource 2. Region-of-interest (ROI) analysis of the PET data was performed using PMOD software (PMOD Technologies Ltd., Version 4.4). Standardized uptake value ratio (SUVR) measures for both FDG and PiB were calculated by averaging unilateral time-activity curves (TACs) and normalizing them to the cerebellar grey matter TAC. For the PiB and FDG analysis, a composite mask was utilized, including the orbitofrontal cortex (OFC), insula, anterior cingulate cortex (AC), mid-cingulate cortex (MC), and posterior cingulate cortex (PC). A global mask was also applied, with details available in online resource 3. Additionally, voxel-wise analysis of the relationship between PiB- and FDG-SUVR, adjusted for age and gender, was conducted using VoxelStats [17]. For a detailed description of the PET analysis, refer to the Online Resource 4. The fMRI analysis was preprocessed and analyzed using the Functional Connectivity Toolbox (CONN version 22.a) in MATLAB R2021b [18], following the default CONN preprocessing pipeline. The ASL data were processed according to the method described by Zhao et al. [19], and diffusion MRI data were analyzed using Tract-Based Spatial Statistics (TBSS) from the FSL software package [20]. Further details regarding the MRI analyses are provided in Online Resource 5, and a schematic overview is presented in Fig. 1.

### Statistical analysis

Regional FDG- and PiB-SUVR values were assessed for normality using the Kolmogorov-Smirnov test in GraphPad Prism 10.0.3 (GraphPad Inc.). Most regional PiB- and

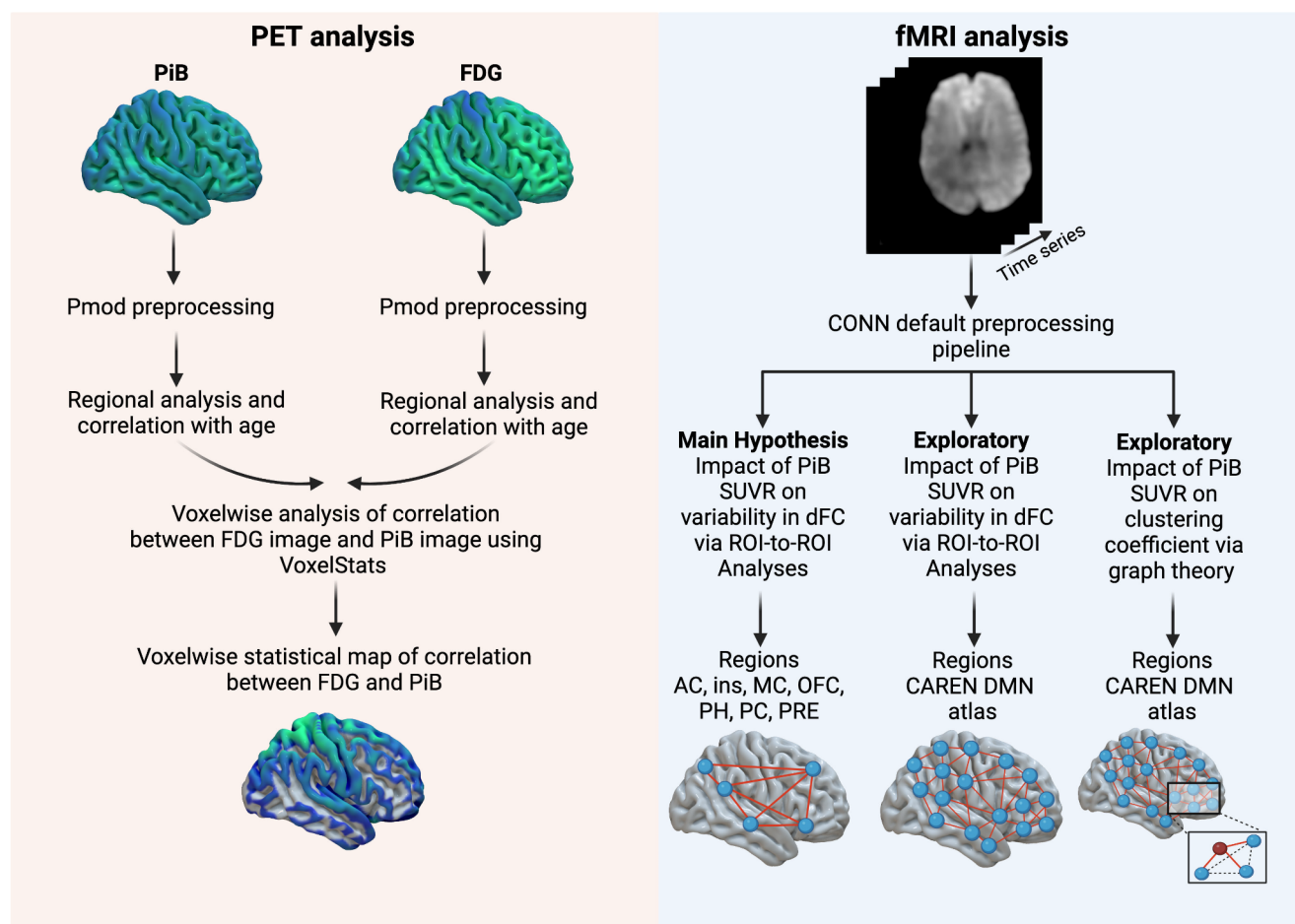


**Fig. 1** Schematic overview of the PET and fMRI analysis. Anterior Cingulate=AC. Insula=ins. Cingulate mid=MC. Precuneus=PRE. Posterior Cingulate=PC. Parahippocampus=PH. Orbito frontal cortex=OFC

FDG-SUVr values were found to deviate from normal distribution (See table in Online Resource 6). Consequently, the Spearman correlation coefficient, as recommended by Kowalski et al. [21], was employed to evaluate the correlation between age and FDG- and PiB-SUVr and subsequently the testing of statistical significance.

## Results

### A $\beta$ -deposition

Initially, we explored the correlation between age and A $\beta$ -deposition (Fig. 2). All included regions exhibited a positive correlation between A $\beta$ -deposition and age, suggesting an accumulation of A $\beta$  with increasing age (Table 1). The composite, global, MC, parahippocampus, and PC demonstrated the highest regional correlation coefficients, indicative of a moderate positive correlation strength (i.e. correlation coefficient > 0.4). In contrast, the remaining regions showed a statistically non-significant and weak

positive correlation between A $\beta$ -deposition and age, especially the hippocampus, paracentral lobule and precuneus.

### Glucose metabolism

Following this, we conducted an evaluation of the correlation between age and FDG-SUVr (Fig. 3). All regions exhibited a negative correlation between FDG-SUVr and age, implying a decline in glucose metabolism with increasing age (Table 1). Specifically, the AC, composite, global, insula, MC, OFC, and precentral gyrus demonstrated a moderate negative correlation with age. In contrast, the hippocampus, paracentral lobule, parahippocampus, PC, and precuneus showed a weak negative correlation strength.

### The influence of A $\beta$ -deposition on glucose metabolism

After establishing the negative correlation of FDG-SUVr with age and the positive correlation of A $\beta$ -deposition with age, both showing spatial dependence, we explored the

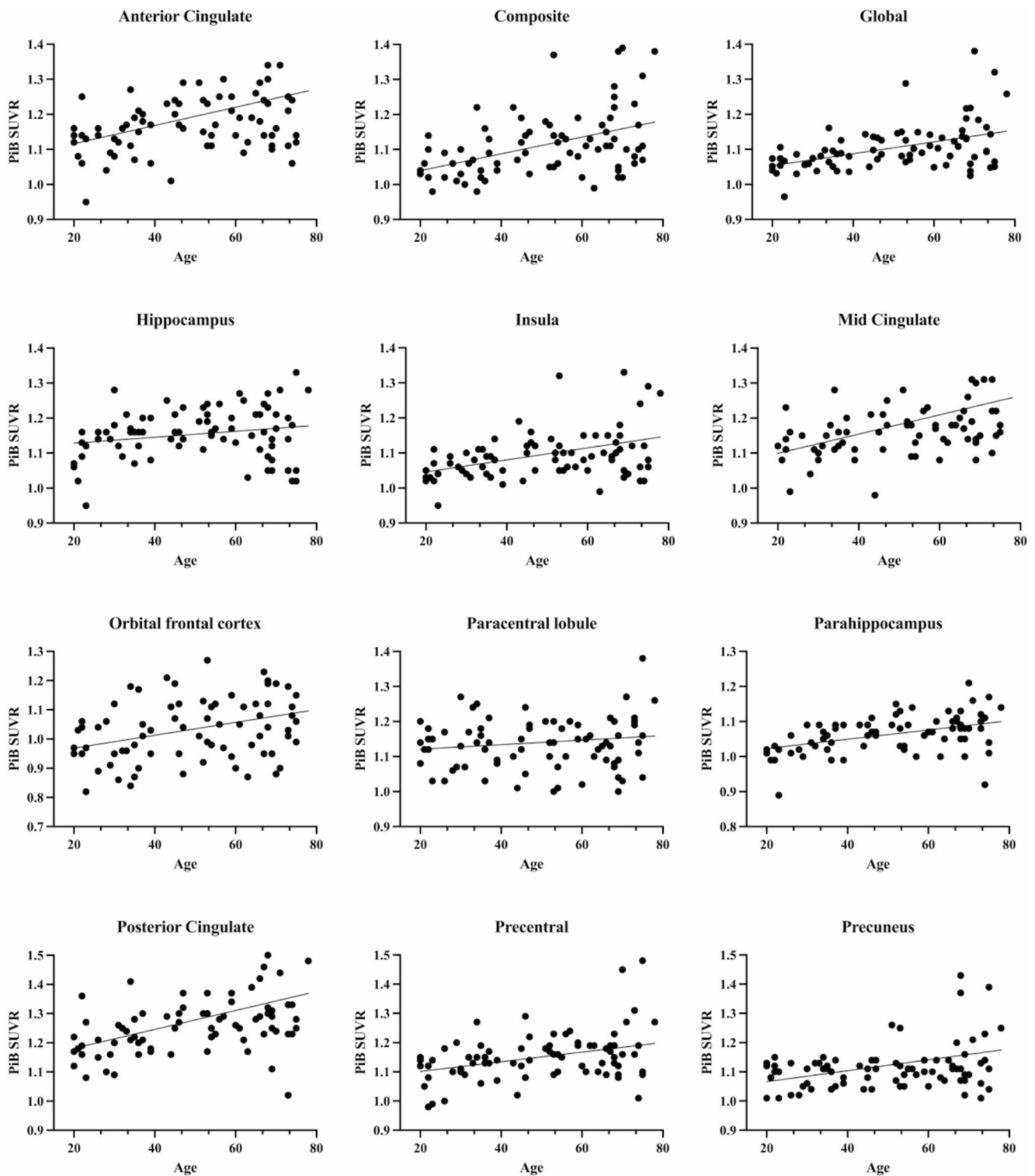


**Fig. 2** The correlation between A $\beta$ -deposition and age

correlation between PiB- and FDG-SUVr while correcting for age and gender. Voxel-wise analysis (Fig. 4) revealed regions with a negative relationship (A $\beta$  increases as glucose metabolism decreases) and regions with a positive

relationship (both A $\beta$  and glucose metabolism increase). Regions showing significant correlations included the MC, OFC, insula, parahippocampus, and precuneus (positive correlation), and the AC and paracentral lobule (negative

**Table 1** Median PiB-SUVr and FDG-SUVr, along with the corresponding Spearman correlation coefficient with age and p-value. Values are presented with 95% confidence interval in parentheses

Region	Median	Spearman <i>r</i>	<i>p</i> -value
<b>PiB</b>			
Anterior cingulate	1.170 (1.14 1.20)	0.375 (0.16 0.55)	0.0007
Composite	1.100 (1.07 1.12)	0.436 (0.23 0.60)	<0.0001
Global	1.089 (1.08 1.11)	0.419 (0.21 0.59)	0.0001
Hippocampus	1.160 (1.14 1.17)	0.175 (-0.05 0.39)	0.1240
Insula	1.080 (1.06 1.10)	0.342 (0.12 0.53)	0.0020
Mid cingulate	1.160 (1.14 1.18)	0.466 (0.27 0.63)	<0.0001
Orbitofrontal cortex	1.030 (0.98 1.06)	0.303 (0.08 0.49)	0.0066
Paracentral lobule	1.140 (1.12 1.16)	0.108 (-0.12 0.33)	0.3447
Parahippocampus	1.070 (1.05 1.08)	0.445 (0.24 0.61)	<0.0001
Posterior cingulate	1.250 (1.23 1.29)	0.479 (0.28 0.64)	<0.0001
Precentral gyrus	1.150 (1.13 1.16)	0.297 (0.07 0.49)	0.0080
Precuneus	1.110 (1.09 1.12)	0.225 (-0.01 0.43)	0.0462
<b>FDG</b>			
Anterior cingulate	1.023 (1.01 1.04)	-0.423 (-0.59 -0.22)	0.0001
Composite	1.179 (1.16 1.20)	-0.524 (-0.67 -0.33)	<0.0001
Global	1.135 (1.12 1.15)	-0.580 (-0.71 -0.41)	<0.0001
Hippocampus	0.773 (0.76 0.79)	-0.105 (-0.33 0.13)	0.3598
Insula	1.109 (1.06 1.13)	-0.683 (-0.79 -0.54)	<0.0001
Mid cingulate	1.259 (1.23 1.28)	-0.533 (-0.68 -0.35)	<0.0001
Orbitofrontal cortex	1.160 (1.13 1.18)	-0.510 (-0.66 -0.32)	<0.0001
Paracentral lobule	1.071 (1.04 1.09)	-0.149 (-0.37 0.08)	0.1935
Parahippocampus	0.832 (0.81 0.85)	-0.166 (-0.38 0.07)	0.1470
Posterior cingulate	1.412 (1.36 1.44)	-0.225 (-0.43 0.04)	0.0479
Precentral gyrus	1.208 (1.186 1.25)	-0.664 (-0.77 -0.51)	<0.0001
Precuneus	1.247 (1.21 1.28)	-0.260 (-0.46 0.03)	0.0215

correlation) (Fig. 4). Generally, temporal regions showed mainly negative correlations, while occipital, frontal, and parietal regions exhibited positive correlations between A $\beta$  and glucose metabolism.

### Influence of A $\beta$ -deposition on brain connectivity

We aimed to explore the links between A $\beta$ -deposition and seed-based dFC within DMN regions to investigate A $\beta$ -depositions impact on neural communication. We found a significant positive correlation between DMN A $\beta$ -deposition and dFC variability from the AC, insula, OFC, and parahippocampus seed-regions (Fig. 5A), suggesting that increased A $\beta$ -deposition in the DMN is linked to fluctuations in FC strength (Table in Online Resource 7). An exploratory analysis of all DMN regions, according to the CAREN DMN atlas [22], reaffirmed these findings, identifying a cluster comprising the insula, OFC, rectus, superior temporal, and temporal pole (cluster *p*-FDR=0.02477) (Fig. 5B and Online Resource 8). Further analysis showed a significant positive correlation between the clustering coefficient and DMN A $\beta$ -deposition in the left insula (*p*-FDR=0.00076), indicating that higher A $\beta$ -deposition

increases the insula's interconnectivity with adjacent structures (Online Resource 9).

### Age and A $\beta$ -depositions influence on FA

We initially explored whether FA decreases with age. As anticipated, the results revealed widespread decreases in FA with advancing age (Online Resource 10), indicating a negative correlation between FA and age. Subsequently, we examined whether A $\beta$  was associated with decreases in FA while adjusting for gender and age. However, this analysis yielded no significant results (nearest *p*=0.274).

### Age and A $\beta$ -depositions influence on CBF

We also investigated the relationship between age and CBF using ASL MRI. As expected, the findings revealed brain-wide decreases in CBF with advancing age (Online Resource 11), suggesting a negative correlation between CBF and age. Subsequently, we assessed the influence of A $\beta$  on CBF, while controlling for gender and age. Nevertheless, the analysis produced non-significant findings, with the closest observed *p*-value being 0.260 located in the right precuneus.

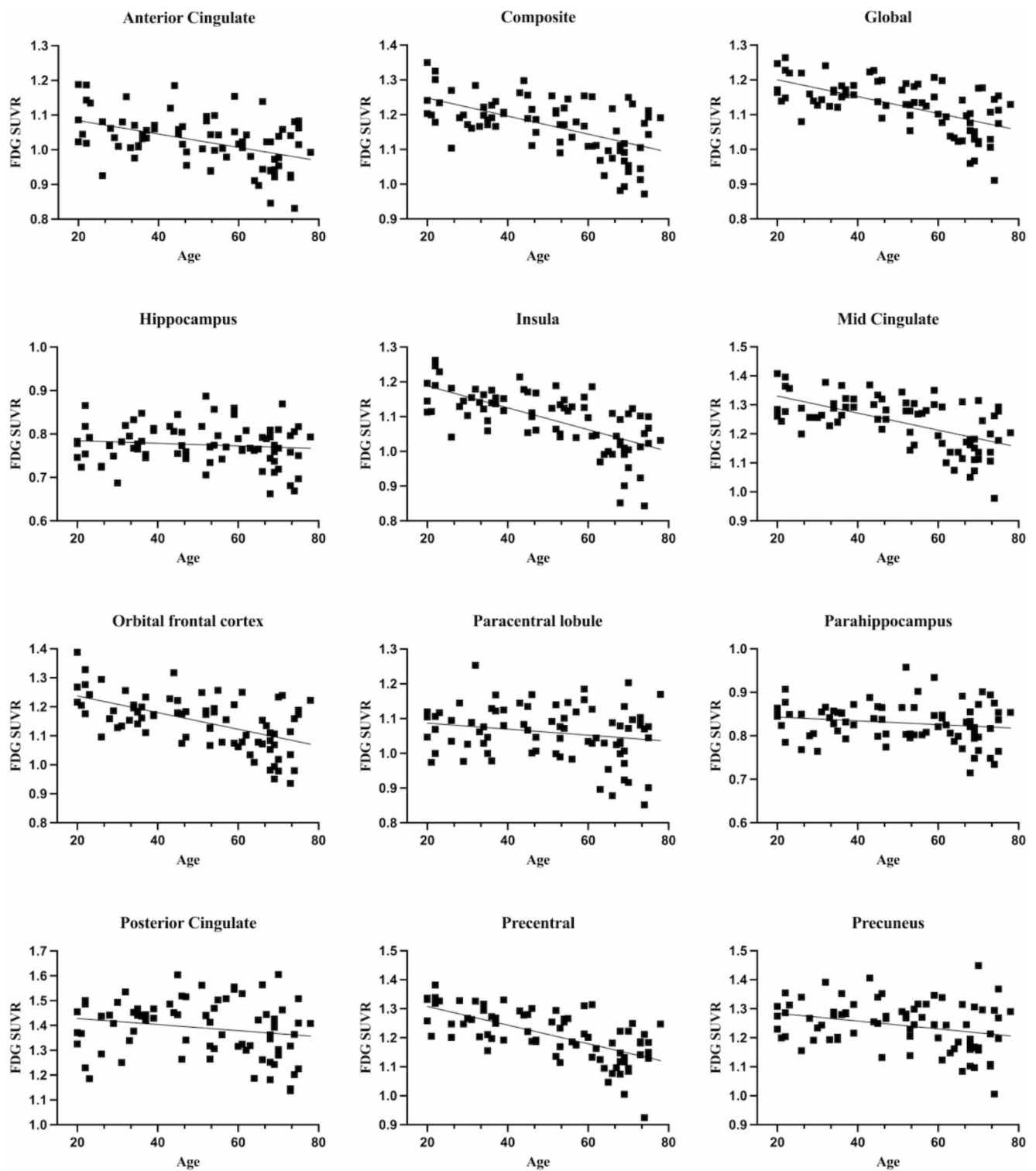
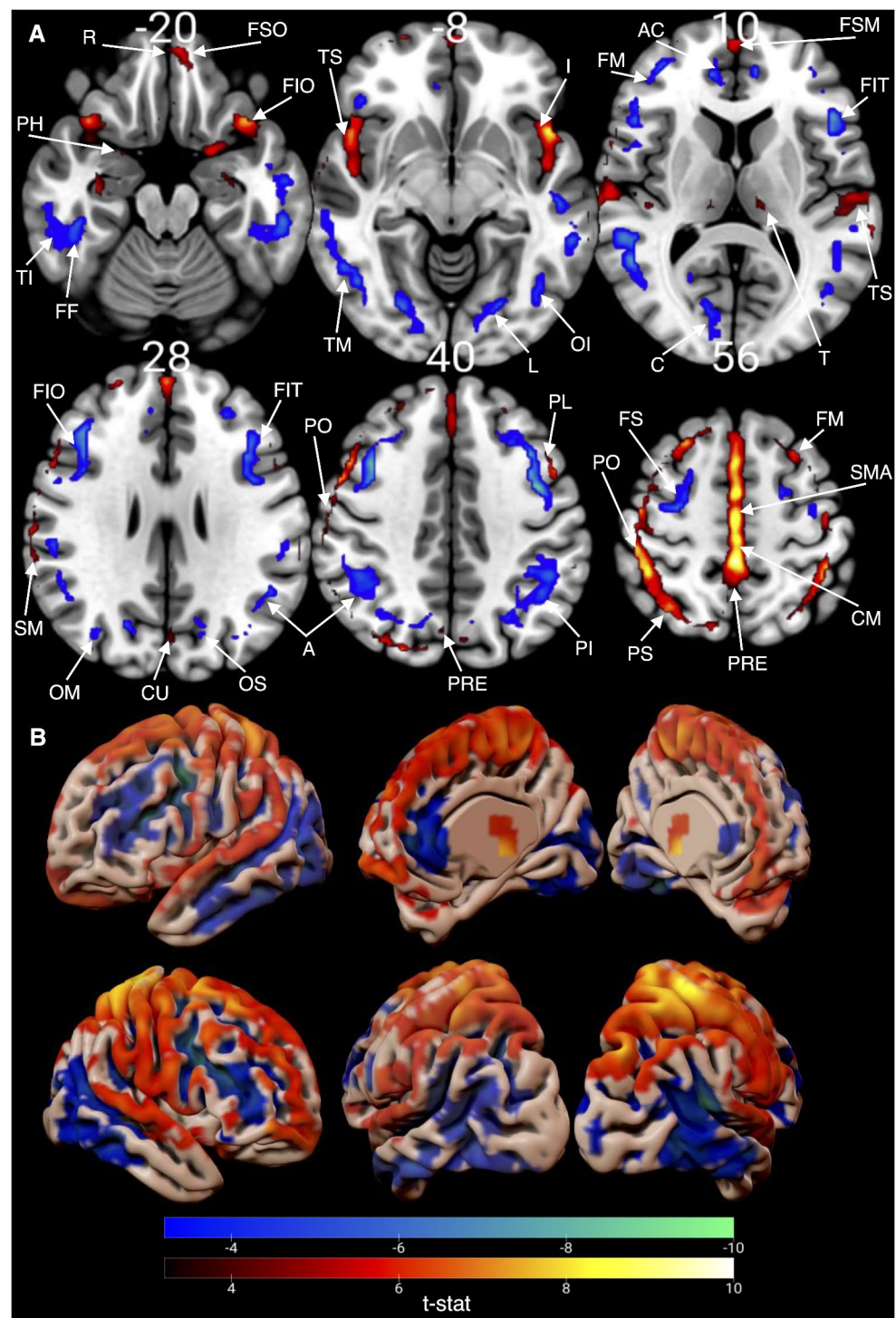


**Fig. 3** The correlation between glucose metabolism and age



**Fig. 4** Correlation between glucose metabolism and A $\beta$ -deposition. Significant multiple comparison corrected t-stat map depicting the voxel-wise correlation between PiB- and FDG-SUVr. The negative t-values displayed in blue-green demonstrate the statistically significant negative correlation between PiB- and FDG-SUVr. The positive t-values displayed in red-yellow demonstrate the positive correlation between PiB- and FDG-SUVr. (A) the statistical maps are presented in axial slices, and regions are marked based on the AAL atlas. (B) the statistical map is illustrated in surface-space for a clearer overview. Rectus=R. Frontal superior orbital=FSO. Parahippocampus=PH. Frontal inferior orbital=FSI. Temporal inferior=TI. Fusiform=FF. Temporal mid=TM. Frontal medial orbital=FMO. Anterior Cingulate=AC. Insula=I. Temporal superior=TS. Lingual=L. Occipital inferior=OI. Frontal superior medial=FSM. Frontal mid=FM. Frontal inferior tri=FIT. Calcarine Fissure=CF. Thalamus=T. Frontal inferior oper=FIO. Supramarginal=SM. Angular=A. Occipital Mid=OM. Cuneus=CU. Occipital superior=OS. Parietal inferior=PI. Parietal superior=PS. Precuneus=PRE. Frontal superior=FS. Cingulate mid=MC. Paracentral lobule=PL. Postcentral=PO. Supplementary motor area=SMA



## Discussion

The present study provides both confirmatory evidence and novel insights, enriching the current understanding in the field. First, we expand on the rare scientific documentation concerning A $\beta$ -deposition in healthy aging. We demonstrate that global A $\beta$ -deposition increases linearly

with age and prove that this accumulation is spatially dependent. Moreover, we also confirm that global glucose metabolism decreases with age and that is also spatially dependent. Additionally, we illustrate an interesting and complex relationship between cerebral A $\beta$ -deposition and glucose metabolism, where some brain regions exhibit positive while other regions demonstrate negative correlations.

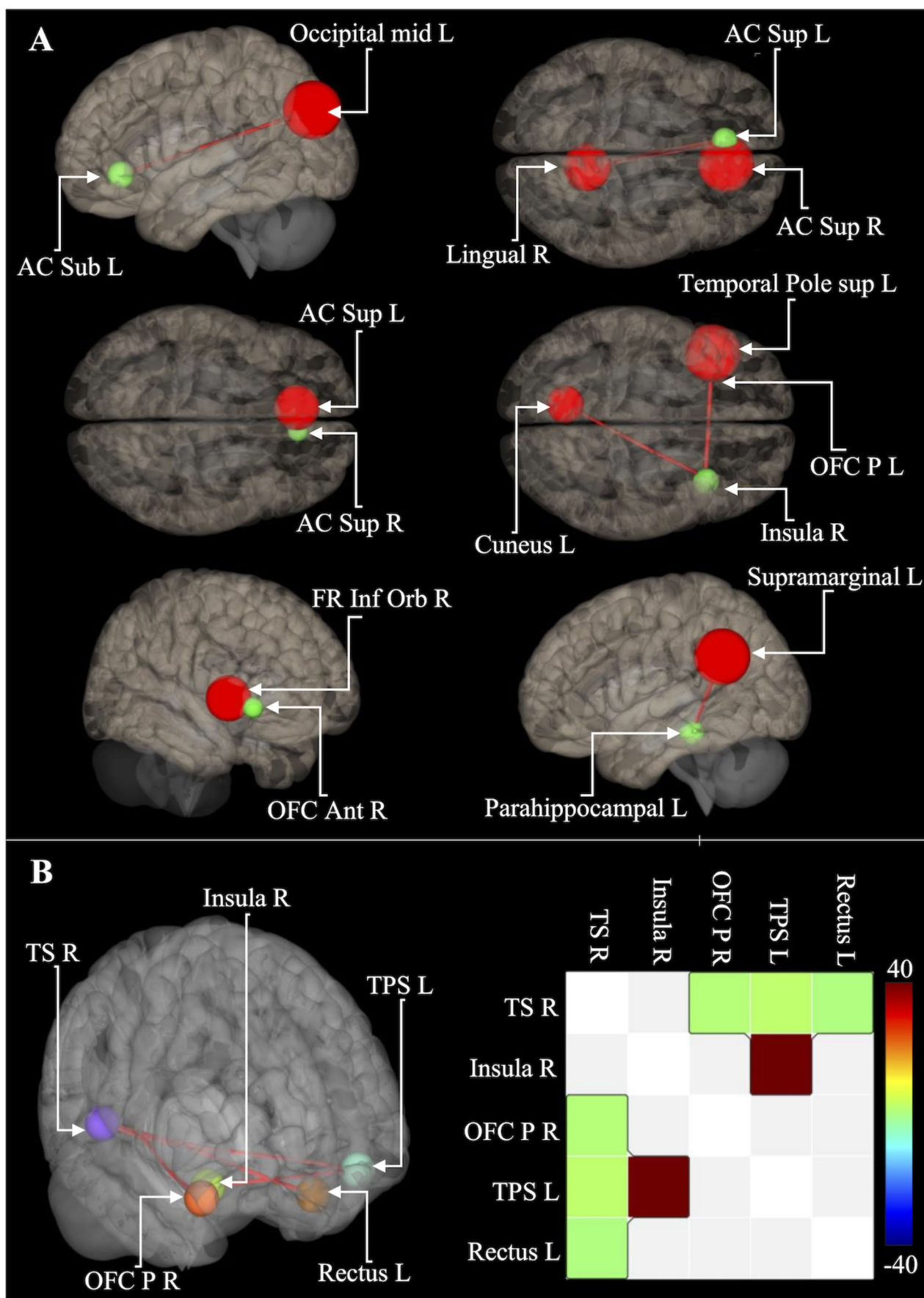




**Fig. 5** Results from the fMRI analysis. **(A)** Regions demonstrating a significant correlation between DMN A $\beta$ -deposition and dFC variability. Green regions represent the seed-region, and the regions associated with changed dFC variability are marked in red. **(B)** Results from the analysis of all regions of the CAREN DMN atlas and related correlation matrix. The color scale represents the threshold-free-cluster-enhancement statistics. Anterior cingulate subgenual=AC sub. Anterior cingulate cortex Superior=AC sup. Orbito frontal cortex posterior=OFC post. Frontal inferior orbital=FR Inf Orb. Orbito frontal cortex anterior=OFC Ant. Temporal Superior R=TS R. Left=L. Right=R

Furthermore, we demonstrate that A $\beta$ -deposition is not only related to glucose metabolism but also neural communication between brain structures. Lastly, we shed light on the state of cerebral blood flow during the process of healthy aging.

### Correlation between A $\beta$ -deposition and age

Our findings align with existing literature on A $\beta$ -deposition across a broad age range of healthy controls. Rodrigue et al. [5] reported a significant positive correlation between age and A $\beta$ -deposition, especially in the precuneus, PC, temporal cortex, and AC. Our study shows similar trends in the AC, PC, and to a lesser extent, the precuneus. Additional analysis revealed that A $\beta$ -depositions in the PC, MC, parahippocampus, and global/composite masks positively correlate with age. Our correlation coefficients are close to Rodrigue et al.'s, except for the precuneus (0.225 vs. 0.41). We believe this discrepancy is due to Rodrigue et al.'s inclusion of A $\beta$ -positive subjects, all of whom are over 70 years old, which likely skews the correlation upward. Oppositely, we excluded one subject with abnormally high SUVRs using the Interquartile Range method for outlier detection, which may account for the slight disparity.

### Correlation between glucose metabolism and age

The FDG-SUVR results demonstrated a negative correlation between cerebral glucose metabolism and age, consistent with existing cross-sectional [23] and longitudinal [24] studies linking decreased glucose metabolism to aging. Our findings mirror this, with the AC, OFC, and precentral gyrus showing strong negative correlations, while posterior regions like the precuneus and PC demonstrate weaker correlations. We also found a strong negative correlation in the insula, which has not been examined in prior studies. However, recent research suggests the insula is an early site of A $\beta$ -deposition [14, 16], indicating it may be sensitive to age-related metabolic changes.

### Correlation between glucose metabolism and A $\beta$ -deposition

We documented a negative correlation between PiB- and FDG-SUVR during healthy aging. Since aging is a risk factor for mild cognitive impairment (MCI) and AD, these findings may help understand AD progression. Both decreases and increases in brain glucose metabolism have been observed in early AD stages. For example, a study on subjective cognitive decline (SCD) patients, the earliest part of the AD continuum, showed hypometabolism in the right middle temporal gyrus (RMTG) and hypermetabolism in occipital regions compared to healthy controls [25]. The voxel-wise analysis of the correlation between PiB-SUVR and FDG-SUVR revealed similar spatial patterns. Specifically, the temporal regions showed predominantly negative correlations, indicating that higher PiB-SUVR levels were associated with lower FDG-SUVR levels. In contrast, the occipital and parietal regions primarily exhibited positive correlations (Fig. 4). Given the correlation between SCD and elevated A $\beta$ -deposition [26], it is plausible that A $\beta$ -deposition causes hypermetabolism in early AD stages or aging. Similarly, individuals in advanced AD stages also demonstrate hypermetabolism [27–29]. In a study by Ashraf et al. [28] four A $\beta$ -negative and one A $\beta$ -positive individual with MCI showed hypermetabolism in occipital, parietal areas, insula, and postcentral regions. Unlike other MCI individuals who exhibited hypometabolism and progressed to AD, these hypermetabolic subjects did not convert to AD within 18 months and had A $\beta$ -deposition resembling elderly controls. This suggests that hypermetabolism may act as a compensatory mechanism against A $\beta$ -deposition. The brain might increase glucose metabolism to counteract A $\beta$  neurotoxicity, delaying cognitive decline. This hypothesis is supported by another study where healthy elderly subjects with increased A $\beta$ -deposition in the precuneus showed hypermetabolism and improved verbal episodic memory, indicating that hypermetabolism helps preserve cognitive function temporarily [30].

### Correlation between A $\beta$ -deposition and brain connectivity

The correlation between increased metabolic activity and excessive A $\beta$ -deposition aligns with fMRI studies showing a positive relationship between A $\beta$ -deposition and neural activation during episodic memory tasks [31]. Studies have found that Tau protein pathology is linked to hypoconnectivity, while A $\beta$ -deposition is associated with increased FC [32–35]. Foster et al. [34] demonstrated that A $\beta$ -deposition levels directly influenced whether hyperconnectivity or hypoconnectivity was observed in the DMN,

with healthy controls showing hyperactivation at slightly elevated A $\beta$ -deposition and hypoactivation at higher levels. Our results demonstrated a positive correlation between A $\beta$ -deposition in the DMN and dFC variability in multiple regions. Enhanced dFC variability, defined as fluctuations in FC between regions, may indicate connectivity reorganization as a compensatory mechanism in defense against A $\beta$  [35]. We also found an increased clustering coefficient in the insula, suggesting heightened local connectivity strength in response to A $\beta$ -deposition. This local hyperconnectivity, interpreted as brain plasticity after neural network damage [36], may serve as a compensatory mechanism to uphold cognitive function. Overall, our results demonstrate a link between A $\beta$ -deposition and alterations in neural communication within the DMN, affecting both FC variability and local neural communication.

### Correlation between FA, age and A $\beta$ -deposition

We observed a pronounced and widespread correlation, between decreasing FA and advancing age, consistent with existing literature [37]. In contrast, no significant correlation was found between FA and A $\beta$ -deposition in our study. While previous research [38] identified such a correlation in cognitively normal elderly individuals with varying A $\beta$ -deposition, the relatively low A $\beta$ -deposition and limited number of elderly subjects in our cohort may explain the absence of a significant correlation.

### Correlation between CBF, age and A $\beta$ -deposition

While our study confirmed a significant and extensive correlation between declining CBF and increasing age, consistent with prior research [39], we did not observe a significant relationship between CBF and A $\beta$ -deposition. Previous studies have documented that A $\beta$ -deposition correlates with increased CBF in various brain regions, such as the insula, caudate, hippocampus, amygdala, frontal, and temporal regions, particularly among elderly A $\beta$ -positive healthy controls [40, 41] (while AD is associated with lower CBF). It is plausible that these findings could have been replicated in our study with a larger cohort, allowing for more comprehensive acquisition of ASL data.

### Limitations

The current study has certain limitations. Firstly, PiB exhibits non-specific binding, including to cerebrovascular amyloid and white matter [42, 43], which complicates PET imaging. Despite this, PiB remains the gold standard for amyloid imaging due to its relatively low non-specific binding [44–47]. Secondly, at the start of our study, 17 subjects

underwent a battery of neuropsychological and cognitive tests, including the Mini-Mental State Examination (MMSE), Clinical Dementia Rating (CDR), Alzheimer's Disease Assessment Scale–Cognitive Subscale (ADAS-cog), and The Montreal Cognitive Assessment (MoCA). However, these tests were discontinued due to their length, which caused fatigue and discomfort among participants during the approximately three-hour scanning procedure. This led to movement-related artifacts and, in some cases, early withdrawal. Logistical constraints also prevented participants from returning for follow-up cognitive assessments. Importantly, none of the 17 subjects showed abnormal cognitive scores, as all were referred to us as healthy by their physicians. We believe these limitations do not significantly bias our results for several reasons. First, all participants were assessed as neurologically and psychiatrically healthy, based on information from their personal physicians and brief evaluations by our departmental physician, which included a conversation about the participants' medical history and medication use, as well as an inspection of scans to confirm the absence of irregularities. Additionally, cognitive impairments are more commonly associated with tau pathology in the middle and later stages of the AD continuum [11, 48–50], making it unlikely that early-stage cognitive issues would be present in this cohort.

### Conclusions

Our study reveals a novel correlation between A $\beta$ -deposition and hypermetabolism in healthy elderly controls, a phenomenon linked to early AD stages. This A $\beta$ -deposition is correlated with alterations in neuronal activity (metabolism) and neural communication, possibly serving as a compensatory mechanism to maintain cognitive function. The insula showed the strongest negative correlation between glucose metabolism and age, indicating its vulnerability to aging. We also found a positive correlation between glucose metabolism and A $\beta$ -deposition in the insula, supported by fMRI results showing altered dFC variability. The insula was the only region with a notable correlation between A $\beta$ -deposition and clustering coefficient, suggesting a compensatory mechanism to maintain its sensory, emotional, motivational, and cognitive functions. Collectively, our results suggest the insula is particularly susceptible to aging and A $\beta$ -deposition in the early phase of the AD continuum, playing a more significant role in aging and AD development than previously recognized.

**Supplementary Information** The online version contains supplementary material available at <https://doi.org/10.1007/s00259-025-07100-w>.

**Acknowledgements** We extend our thanks to our dedicated healthy participants that despite our lengthy experiments helped us for the sake of science and the personnel from the Nuclear Medicine department at Odense University Hospital and the study team contributing to this research.

**Author contributions** MSV conceptualized, designed, and initiated the study. MSV and LVK conducted the PET/MRI scans. LVK performed the data analysis and drafted the first version of the manuscript. MSV and TSM revised the manuscript and supervised LVK. ZAF quality controlled the MRI and PET scans of the subjects to exclude any subject suspicious of brain trophy. All authors read and approved the final version of the manuscript.

**Funding** Open access funding provided by Odense University Hospital. The study was supported by the Grant #188308 from the Psychiatry in the Southern Region of Denmark (Mental Health Service) and Grant #324901 from Free Research Fund from the Southern Region of Denmark.

**Data availability** The data from this study are currently stored in a secure database owned by the University of Southern Denmark. This data may be shared with qualified investigators for non-commercial purposes, subject to restrictions regarding participant consent and data protection legislation.

## Declarations

**Competing interests** The authors declare no conflict of interest.

**Ethics approval** This study was performed in line with the principles of the Declaration of Helsinki. Approval was granted by the Ethics Committee of the southern region of Denmark.

**Consent to participate** Informed consent was obtained from all individual participants included in the study.

**Consent for publication** Written informed consent was obtained from every participant.

**Open Access** This article is licensed under a Creative Commons Attribution 4.0 International License, which permits use, sharing, adaptation, distribution and reproduction in any medium or format, as long as you give appropriate credit to the original author(s) and the source, provide a link to the Creative Commons licence, and indicate if changes were made. The images or other third party material in this article are included in the article's Creative Commons licence, unless indicated otherwise in a credit line to the material. If material is not included in the article's Creative Commons licence and your intended use is not permitted by statutory regulation or exceeds the permitted use, you will need to obtain permission directly from the copyright holder. To view a copy of this licence, visit <http://creativecommons.org/licenses/by/4.0/>.

## References

- McDonald RB. Basic concepts in the Biology of Aging. Biology of Aging. CRC: Boca Raton.; 2019. pp. 1–36.
- Michael T, Beal F. 'Mitochondrial dysfunction and oxidative stress in neurodegenerative disease'. Nat Rev, 443, 2006.
- Malén T et al. Jul., 'Atlas of type 2 dopamine receptors in the human brain: Age and sex dependent variability in a large PET cohort', Neuroimage, vol. 255, 2022, <https://doi.org/10.1016/j.neuroimage.2022.119149>
- Karrer TM, McLaughlin CL, Guaglianone CP, Samanez-Larkin GR. 'Reduced serotonin receptors and transporters in normal aging adults: a meta-analysis of PET and SPECT imaging studies', Neurobiol Aging, vol. 80, pp. 1–10, Aug. 2019, <https://doi.org/10.1016/j.neurobiolaging.2019.03.021>
- Rodrigue K et al. 'Beta-Amyloid burden in healthy aging', Neurology, vol. 78, pp. 387–395, 2012, [Online]. Available: [www.neurology.org](http://www.neurology.org).
- Raichle ME, Gusnard DA. Appraising the brain's energy budget. Proc Natl Acad Sci U S A. 2002;99(16):10237–9. <https://doi.org/10.1073/pnas.172399499>.
- Itoh M et al. 'Stability of cerebral blood flow and oxygen metabolism during normal aging', Gerontology, 36, 1, pp. 43–8, 1990, <https://doi.org/10.1159/000213174>
- Landau SM et al. Jul., 'Associations between cognitive, functional, and FDG-PET measures of decline in AD and MCI', Neurobiol Aging, vol. 32, no. 7, pp. 1207–1218, 2011, <https://doi.org/10.1016/j.neurobiolaging.2009.07.002>
- Nichols E, et al. Estimation of the global prevalence of dementia in 2019 and forecasted prevalence in 2050: an analysis for the global burden of Disease Study 2019. Lancet Public Health. 2022;7(2):e105–25. [https://doi.org/10.1016/S2468-2667\(21\)00249-8](https://doi.org/10.1016/S2468-2667(21)00249-8).
- Hardy JA, Higgins GA. 'Alzheimer's Disease: The Amyloid Cascade Hypothesis', Science (1979), vol. 256, no. 5054, 1992.
- Pichet Binette A, et al. Amyloid-associated increases in soluble tau relate to tau aggregation rates and cognitive decline in early Alzheimer's disease. Nat Commun. 2022;13(1):6635. <https://doi.org/10.1038/s41467-022-34129-4>.
- Jansen WJ, et al. Prevalence of cerebral amyloid pathology in persons without dementia: a meta-analysis. JAMA - J Am Med Association. 2015;313:1924–38. <https://doi.org/10.1001/jama.2015.4668>.
- Klunk WE, et al. Imaging brain amyloid in Alzheimer's Disease with Pittsburgh Compound-B. Ann Neurol. 2004;55(3):306–19. <https://doi.org/10.1002/ana.20009>.
- Collij LE et al. 'Multitracer model for staging cortical amyloid deposition using PET imaging', Neurology, vol. 95, no. 11, pp. E1538–E1553, 2020, <https://doi.org/10.1212/WNL.00000000000010256>
- Palmqvist S, et al. Earliest accumulation of  $\beta$ -amyloid occurs within the default-mode network and concurrently affects brain connectivity. Nat Commun. 2017;8(1). <https://doi.org/10.1038/s41467-017-01150-x>.
- Mattsson N, Palmqvist S, Stomrud E, Vogel J, Hansson O. Staging  $\beta$ -Amyloid Pathology with amyloid Positron Emission Tomography. JAMA Neurol. 2019;76(11):1319–29. <https://doi.org/10.1001/jamaneurol.2019.2214>.
- Mathotaarachchi S, et al. VoxelStats: a MATLAB package for multi-modal voxel-wise brain image analysis', Front Neuroinform. No JUNE. 2016;10:1–12. <https://doi.org/10.3389/fninf.2016.00020>.
- Nieto-Castanon A, Whitfield-Gabrieli S. CONN functional connectivity toolbox: RRID SCR\_009550, release 22. CONN Funct Connectivity Toolbox: RRID SCR\_009550 Release 22. 2022. <https://doi.org/10.5644/hilbertpress.2246.5840>.
- Zhao MY, et al. A systematic study of the sensitivity of partial volume correction methods for the quantification of perfusion from pseudo-continuous arterial spin labeling MRI. NeuroImage. 2017;162:384–97. <https://doi.org/10.1016/j.neuroimage.2017.08.072>.

20. Smith SM et al. 'Tract-based spatial statistics: Voxelwise analysis of multi-subject diffusion data', *Neuroimage*, vol. 31, no. 4, pp. 1487–1505, 2006, <https://doi.org/10.1016/j.neuroimage.2006.02.024>
21. Kowalski CJ. On the effects of Non-normality on the distribution of the Sample product-moment correlation coefficient. *Appl Stat.* 1972;21(1). <https://doi.org/10.2307/2346598>.
22. Doucet GE, Lee WH, Frangou S. Evaluation of the spatial variability in the major resting-state networks across human brain functional atlases. *Hum Brain Mapp.* 2019;40(15):4577–87. <https://doi.org/10.1002/hbm.24722>.
23. Kakimoto A, Ito S, Okada H, Nishizawa S, Minoshima S, Ouchi Y. Age-related sex-specific changes in brain metabolism and morphology. *J Nucl Med.* 2016;57(2):221–5. <https://doi.org/10.2967/jnumed.115.166439>.
24. Ishibashi K, Onishi A, Fujiwara Y, Oda K, Ishiwata K, Ishii K. Longitudinal effects of aging on 18F-FDG distribution in cognitively normal elderly individuals. *Sci Rep.* 2018;8(1):1–8. <https://doi.org/10.1038/s41598-018-29937-y>.
25. Dong QY, Li TR, Jiang XY, Wang XN, Han Y, Jiang JH. Glucose metabolism in the right middle temporal gyrus could be a potential biomarker for subjective cognitive decline: a study of a Han population. *Alzheimers Res Ther.* 2021;13(1):1–12. <https://doi.org/10.1186/s13195-021-00811-w>.
26. Amariglio RE et al. 'Subjective cognitive complaints and amyloid burden in cognitively normal older individuals', *Neuropsychologia*, vol. 12, no. 50, pp. 2880–2886, 2012, <https://doi.org/10.1016/j.neuropsychologia.2012.08.011>. Subjective
27. Cohen AD, et al. Basal cerebral metabolism may modulate the cognitive effects of A $\beta$  in mild cognitive impairment: an example of brain reserve. *J Neurosci.* 2009;29(47):14770–8. <https://doi.org/10.1523/JNEUROSCI.3669-09.2009>.
28. Ashraf A, Fan Z, Brooks DJ, Edison P. Cortical hypermetabolism in MCI subjects: a compensatory mechanism? *Eur J Nucl Med Mol Imaging.* 2015;42(3):447–58. <https://doi.org/10.1007/s00259-014-2919-z>.
29. Croteau E, et al. A cross-sectional comparison of brain glucose and ketone metabolism in cognitively healthy older adults, mild cognitive impairment and early Alzheimer's disease. *Exp Gerontol.* 2018;107:18–26. <https://doi.org/10.1016/j.exger.2017.07.004>.
30. Ossenkoppele R, Madison C, Oh H, Wirth M, Van Berckel BNM, Jagust WJ. 'Is verbal episodic memory in elderly with amyloid deposits preserved through altered neuronal function?', *Cerebral Cortex*, 24, 8, pp. 2210–8, 2014, <https://doi.org/10.1093/cercor/bht076>
31. Mormino EC, Brandel MG, Madison CM, Marks S, Baker SL, Jagust WJ. 'A $\beta$  Deposition in aging is associated with increases in brain activation during successful memory encoding', *Cerebral Cortex*, vol. 22, no. 8, pp. 1813–1823, 2012, <https://doi.org/10.1093/cercor/bhr255>
32. Jorge S, Mert RS, Quanzheng L, Georges EF, Reisa S, Keith AJ. 'Tau and A $\beta$  proteins distinctively associate to Functional Network changes in the aging brain', *Alzheimers Dement*, 13, 11, pp. 1261–9, 2017, <https://doi.org/10.1016/j.jalz.2017.02.011>. Tau
33. Schultz AP, et al. Phases of hyperconnectivity and hypoconnectivity in the default mode and salience networks track with amyloid and tau in clinically normal individuals. *J Neurosci.* 2017;37(16):4323–31. <https://doi.org/10.1523/JNEUROSCI.3263-16.2017>.
34. Foster CM, Kennedy KM, Horn MM, Hoagey DA, Rodrigue KM. 'Both hyper- and hypo-activation to cognitive challenge are associated with increased beta-amyloid deposition in healthy aging: A nonlinear effect', *Neuroimage*, vol. 166, no. October 2017, pp. 285–292, 2018. <https://doi.org/10.1016/j.neuroimage.2017.10.068>
35. Hahn A et al. 'Association between earliest amyloid uptake and functional connectivity in cognitively unimpaired elderly', *Cerebral Cortex*, vol. 29, no. 5, pp. 2173–2182, 2019, <https://doi.org/10.1093/cercor/bhz020>
36. Li K et al. 'Aberrant functional connectivity network in subjective memory complaint individuals relates to pathological biomarkers', *Transl Neurodegener.* vol. 7, no. 1, pp. 1–10, 2018, <https://doi.org/10.1186/s40035-018-0130-z>
37. Lawrence KE, et al. Age and sex effects on advanced white matter microstructure measures in 15,628 older adults: a UK biobank study. *Brain Imaging Behav.* 2021;15(6):2813–23. <https://doi.org/10.1007/s11682-021-00548-y>.
38. Vipin A, et al. Amyloid burden accelerates white matter degradation in cognitively normal elderly individuals. *Hum Brain Mapp.* 2019;40(7):2065–75. <https://doi.org/10.1002/hbm.24507>.
39. Mokhber N, et al. Cerebral blood flow changes during aging process and in cognitive disorders: a review. *Neuroradiol J.* 2021;34(4):300–7. <https://doi.org/10.1177/19714009211002778>.
40. Fazlollahi A, et al. Increased cerebral blood flow with increased amyloid burden in the preclinical phase of alzheimer's disease. *J Magn Reson Imaging.* 2020;51(2):505–13. <https://doi.org/10.1002/jmri.26810>.
41. Bangen KJ et al. 'Cerebral blood flow and amyloid- $\beta$  interact to affect memory performance in cognitively normal older adults', *Front Aging Neurosci.* vol. 9, no. JUN, pp. 1–14, 2017, <https://doi.org/10.3389/fnagi.2017.00181>
42. Coomans EM et al. 'Genetically identical twin-pair difference models support the amyloid cascade hypothesis', *Brain*, vol. 146, no. 9, pp. 3735–3746, 2023, <https://doi.org/10.1093/brain/awad077>
43. Moghbel MC, et al. Amyloid- $\beta$  imaging with PET in Alzheimer's disease: is it feasible with current radiotracers and technologies? *Eur J Nucl Med Mol Imaging.* 2012;39(2):202–8. <https://doi.org/10.1007/s00259-011-1960-4>.
44. Buccino P, Savio E, Porcal W. Fully-automated radiosynthesis of the amyloid tracer [11 C] PiB via direct [11 C]CO<sub>2</sub> fixation-reduction. *EJNMMI Radiopharm Chem.* Dec. 2019;4(1). <https://doi.org/10.1186/s41181-019-0065-4>.
45. Quigley H, Colloby SJ, O'Brien JT. PET imaging of brain amyloid in dementia: a review. Oct. 2011. <https://doi.org/10.1002/gps.2640>.
46. Klunk WE et al. 'The Centiloid project: Standardizing quantitative amyloid plaque estimation by PET', *Alzheimer's and Dementia*, vol. 11, no. 1, pp. 1–15.e4, 2015, <https://doi.org/10.1016/j.jalz.2014.07.003>
47. Josef P, Myburgh. Solingapuram. Sai, 'Two decades of [11 C]PiB synthesis, 2003–2023: a review'. *Am J Nucl Med Mol Imaging.* 2024;14(1):48–62. <https://doi.org/10.62347/adsk6584>.
48. Brier MR, et al. Tau and A $\beta$  imaging, CSF measures, and cognition in Alzheimer's disease. 8 338. 2017. <https://doi.org/10.1126/scitranslmed.aaf2362>. Tau.
49. Betthausen TJ, Kosciak RL, Jonaitis EM, Allison SL, Cody KA, Rowley HA, Stone CK, Mueller KD, Clark LR, Carlsson CM, Chin NA, Bradley SA, C T, Johnson SC, Erickson CM. 'Amyloid and tau imaging biomarkers explain cognitive decline from late middle-age', Jan. 01, 2020, Oxford University Press. <https://doi.org/10.1093/brain/awz399>
50. Bennett RE et al. Jul., 'Enhanced Tau Aggregation in the Presence of Amyloid  $\beta$ ', *American Journal of Pathology*, vol. 187, no. 7, pp. 1601–1612, 2017, <https://doi.org/10.1016/j.ajpath.2017.03.011>

**Publisher's note** Springer Nature remains neutral with regard to jurisdictional claims in published maps and institutional affiliations.